DOI:
10.1016/j.ejmech.2016.03.014

Document Version
Peer reviewed version

Accepted Manuscript

Systematic comparison of the mono-, dimethyl- and trimethyl 3-hydroxy-4(1H)-pyridones – attempted optimization of the orally active iron chelator, deferiprone

Yuan-Yuan Xie, Zidong Lu, Xiao-Le Kong, Tao Zhou, Sukhi Bansal, Robert Hider

PII: S0223-5234(16)30188-X

DOI: 10.1016/j.ejmech.2016.03.014

Reference: EJMECH 8439

To appear in: *European Journal of Medicinal Chemistry*

Received Date: 27 November 2015

Revised Date: 3 March 2016

Accepted Date: 4 March 2016

Please cite this article as: Y.-Y. Xie, Z. Lu, X.-L. Kong, T. Zhou, S. Bansal, R. Hider, Systematic comparison of the mono-, dimethyl- and trimethyl 3-hydroxy-4(1H)-pyridones – attempted optimization of the orally active iron chelator, deferiprone, *European Journal of Medicinal Chemistry* (2016), doi: 10.1016/j.ejmech.2016.03.014.

Graphic Abstract

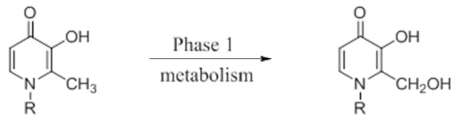

R	Metabolic Hydroxylation
CH_3	fast
H	slow

Systematic comparison of the mono-, dimethyl- and trimethyl 3-hydroxy-4(1H)-pyridones – attempted optimization of the orally active iron chelator, deferiprone

Yuan-Yuan Xie,[a†] Zidong Lu,[b†] Xiao-Le Kong,[b] Tao Zhou,[c] Sukhi Bansal,[b] Robert Hider[b]

[a] College of Pharmaceutical Sciences, Zhejiang University of Technology, Hangzhou, China

[b] Institute of Pharmaceutical Science, King's College London, UK

[c] School of Food Science and Biotechnology, Zhejiang Gongshang University, Hangzhou, China.

[†] Joint first authors.

Abstract

A range of close analogues of deferiprone have been synthesised. The group includes mono-, di- and tri-methyl-3-hydroxy-4(1H)-pyridones. These compounds were found to possess similar pFe^{3+} values to that of deferiprone, with the exception of the 2.5-dimethylated derivatives. Surprisingly the NH-containing hydroxy-4(1H)-pyridones were found to be marginally more lipophilic than the corresponding N-Me containing analogues. This same group are also metabolised less efficiently by Phase 1 hydroxylating enzymes than the corresponding N-Me analogues.

As result of this study, three compounds have been identified for further investigation centred on neutropenia and agranulocytosis.

Corresponding author:

E-mail address: robert.hider@kcl.ac.uk

Highlights:

- Mono-, di- and trimethyl 3-hydroxy-4(1H)-pyridones possess very similar pFe^{3+} values.
- N-methyl-3-hydroxy-4(1H)-pyridones are less lipophilic than corresponding NH- compounds.
- N-methyl-4(1H)-pyridones are metabolised faster than corresponding NH-compounds.

Graphic Abstract

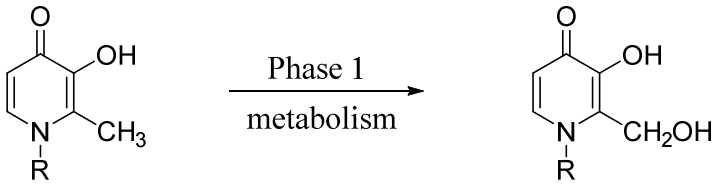

R	**Metabolic Hydroxylation**
CH_3	fast
H	slow

1. Introduction

Deferiprone (**1**) is a useful iron-selective chelator which is widely used to treat systemic iron overload associated with regular blood transfusion.[1,2] It is particularly effective at removing iron from the iron-overloaded heart.[3,4] The free ligand readily enters cells by non facilitated diffusion and the resulting iron complex, by virtue of lacking a charge and possessing a molecular weight of less than 500 is able to efflux from cells, leading to enhanced renal excretion of iron.[5] Deferiprone (**1**) has a low affinity for iron(II) and does not disturb the normal cytosolic labile iron pool.[6] However deferiprone has two disadvantages, namely rapid metabolism[7] and initiation of reversible agranulocytosis in approximately 1% of patients receiving the drug.[8] Metabolism leads to glucuronidation of the 3-hydroxyl function,[7] thereby removing the chelating ability of the molecule. This property leads to relatively high doses of deferiprone being adopted in the clinic, typically 75-100 mg/kg.[9]

There have been several attempts to modify the 3-hydroxy-4(1H)-pyridone structure, while maintaining the same high affinity for iron(III) and limiting the molecular weight of the corresponding iron(III) complex to less than 500. Thus the introduction of an additional nitrogen into the ring leading to the 3-hydroxypyridazin-4-one (**2**) and 5-hydroxypyridazin-4-one (**3**) groups has been investigated.[10] However the introduction of the additional nitrogen, leads to a marked reduction in the affinity for iron(III); the pFe^{3+} values being 20.6, 14.8, 17.2 for **1**, **2** and **3** respectively.[10] In order to successfully scavenge iron from iron overloaded tissues, a minimum pFe^{3+} value of 20 is required.[5] The introduction of fluorine into the hydroxypyridinone structure has been investigated.[11] However the presence of the fluorine was also found to reduce the pFe^{3+} values when compared with that of deferiprone, thus **4**, **5** and **6** have values of 19.4, 17.8 and 18.9 respectively.[12]

In a further attempt to optimize, the logP and pFe^{3+} values of 3-hydroxy-4(1H)-pyridone, together with the rate of metabolism, a range of monomethyl, dimethyl and trimethyl analogues of deferiprone (**7**-**10**) have been investigated, the results of which are reported in this communication.

2. Chemistry

2.1 Synthesis

The synthesis of four of the deferiprone analogues was achieved using previously published methods; namely **7**,[13] **9a**,[7] **10a**[14] and **10b**.[15] Scheme 1 illustrates the synthetic route employed for the preparation of **8a** and **8b** starting from commercially available kojic acid (**11**). Protection of the 3-hydroxyl group was achieved by methylation using dimethyl sulfate or benzylation using benzylchloride, both under basic conditions. The hydroxymethyl function was oxidised to a carboxylic acid, which was subsequently decarboxylated by heating in 1-methyl-2-pyrrolidinone to yield the protected pyrones **14a** and **14b**. The ring oxygen was replaced by nitrogen *via* reaction with aqueous ammonia and the resulting 4(1H)-pyridones were subjected to a Mannich reaction with dimethylamine to yield the 4(1H)-pyridones **16a** and **16b**. Reduction of **16b** yielded **8b** and reduction of **16a** yielded **17**, which on methylation and subsequent treatment with BBr_3 yielded **8a**. The preparation of **9b** was also initiated using kojic acid, which was converted to the 6-methyl-4(1H)-pyridone in a step wise manner (Scheme 2)

3. Results and discussion

3.1 Physicochemical Characterisation.

The pKa and $\log K_{eq}(Fe^{3+})$ values were investigated using an automated spectrophotometric titration system. The UV profile of **8b** over the pH range 1.6-11.0 (Figure 1A) on analysis yielded two pKa values, namely 3.31 (carbonyl) and 9.49 (phenol). When the titration was repeated in the presence of iron(III), over the pH range 1.2-8.0, the visible profile was indicative of three species, FeL, FeL_2 and FeL_3 (Figure 1B). Resolution of the spectra of these three species led to the determination of the corresponding three equilibrium constants, namely; $\log K_1$ = 14.41, $\log\beta_2$ = 26.31 and $\log\beta_3$ =35.80. A speciation plot based on these values is presented in figure 1C. It is clear that under most *invivo* conditions, where **8b** would be present in excess of labile iron, the dominant species is the neutral FeL_3 complex. Analogous titrations for the other hydroxypyridinones reported in this study are presented in the Supplementary Data. All the determined pKa values and affinity

constants for iron(III) are presented in Table 1. The pFe^{3+} value for **8b** was calculated to be 20.06. The mean pFe^{3+} value of the 4 N-methyl compounds, 20.3, is marginally higher than the mean pFe^{3+} values of the 4 N-H compounds, namely 19.9. The pFe^{3+} values of the two 2,5-dimethyl derivatives are the lowest in the series.

All the ligands investigated were found to be hydrophilic (Table 1). The resulting neutral iron(III) complexes were also hydrophilic. The overall relationship between ligands and iron complexes being linear, with a slope of 2.25 (Figure 2); that is the iron complexes are more hydrophilic than the free ligands. This a similar result to that of a more extensive study of hydroxypyridinones.[16] On comparison of the analogous pairs, namely **1**/**7**; **8a**/**8b**; **9a**/**9b** and **10a**/**10b**, without exception, the N-H-containing compounds were found to be less hydrophilic than the N-Me-containing compounds. The same difference occurs with the iron(III) complexes. This is surprising because the N-methyl compounds all contain one more sp_3 carbon atom than the N-H compounds and the N-H compounds all possess a larger hydrophilic surface area. Both these differences suggest that the N-H compounds of each analogous pair would be more hydrophilic than the corresponding N-Me compounds, which contradicts the observed logP values. This entire group of molecules have two mesomeric forms (**22** and **23**) and the percentage contribution of each form will influence the oil/water partitioning properties, the aromatic mesomer (**23**) being zwitterionic. Using DFT simulation[17] we have determined the percentage contribution of each mesomeric form, *in vacuo* and in a simulated aqueous environment, for the four pyridinone pairs. There is a constantly lower contribution from the zwitterionic mesomer of the NH compounds when compared with the corresponding NMe compounds for calculations undertaken both in the presence of water and *in vacuo* (Figure 3). However this difference is small, for instance in the presence of water the average zwitterionic contribution is 31.5 ± 0.7% for the four N-Me compounds and 30.6 ± 0.7% for the four N-H compound. It is unclear whether this difference is suffient to explain the differences in partition coefficients; namely mean logP value for the 4 N-methyl compounds is -0.85, whereas the corresponding value for the N-H compounds is -0.51. In a further

attempt to identify the cause of this difference in partitioning behavior, the possibility of dimer formation *via* aromatic π – π interaction between two hydroxypyridinone molecules was considered. It is established that pyridine-pyridine dimers form parallel-displaced configurations.[18] The zwitterionic nature of the hydroxy-4(1H)-pyridones could favor a similar dimer configuration. Indeed, the presence of a dimer was detected by MS where at 140 μM the ratio of peak heights of the monomer (140.17) and dimer (279.0) for deferiprone (**1**) was 1.12 (Figure 4). In contrast, at the same concentration, the pyridinone **7** only gave a weak dimer peak (251) when compared with the monomer peak (126), the ratio being 0.11. The presence of the dimer is strongly concentration dependent (Figure 5). Thus there is a clear difference in behavior between the N-Me and N-H derivatives with respect to the tendency of dimer formation. However the determined logP values (water/octanol) of deferiprone over the concentration range 200 μM – 10 μM did not change, indicating that the tendency for dimer formation did not influence the partitioning properties of the chelators.

Thus in summary the highest pFe^{3+} values of the entire group is associated with deferiprone (**1**), although the values for **8a** and **9a** are quite close and in excess of 20. The lowest pFe^{3+} values are associated with (**10a**) and (**10b**), this resulting from the markedly higher pKa_2 values than the rest of the group. As indicated above, the logP values of the free ligands are higher for the NH-containing group, **7** having the highest value of those pyridinones with pFe values greater than 20.

3.2 Metabolism of 3-Hydroxy-4(1H)-pyridones

The metabolism of this group of hydroxypyridinones was assessed using human liver microsomes; both phase 1 and phase 2 reactions being monitored. The phase 1 metabolites were characterised by mass spectroscopy. It was not possible to study **9b** using this technique due to complications with dimerisation of the free ligand. The extent of glucuronidation (Phase 2) was found to be similar throughout the entire series (Figure 6). Phase 1 metabolism, was established to be hydroxylation, in agreement with earlier studies.[7,19] **7** and **8b** were found to hydroxylated to a less extent than deferiprone (**1**), indeed all the (N-H)pyridinones were hydroxylated at a

lower rate than the corresponding (N-Me)pyridinones.

4. Conclusion

Despite its success in the treatment of thalassaemia, deferiprone, suffers from extensive metabolism[7] and the initiation of reversible agranulocytosis.[8] Consequently a replacement candidate is required; introduction of either an additional nitrogen in the ring or a fluorine substituent was found to reduce the pFe^{3+} value, which is a critically important parameter for efficient iron scavenging. As deferiprone possesses many ideal properties for the removal of excess iron in biological tissues, in the present study we decided to systematically investigate the properties of a range of close structural analogues. The comparison of pKa, pFe and logP values, together with metabolic profiles, identified several new features of these molecules. Although none of the seven analogues bind iron(III) as tightly as deferiprone, five of them possess pFe^{3+} values > 20, in marked contrast to other close analogues, recently investigated.[10-12] The substitution of the 1-methyl substituent with hydrogen had two beneficial effects, an enhanced logP value and a reduced tendency for phase 1 metabolism. The enhanced logP value is surprising, and remains unexplained at the present time. The critical physicochemical parameters of the three analogues with potential for clinical application, namely **7**, **8b** and **9b**, are pFe^{3+}, 20.17, 20.06 and 20.13 respectively and logP, -0.58, -0.59 and -0.73 respectively. All three are metabolised more slowly than deferiprone *via* the phase 1 route. Although only marginally different to the corresponding values for deferiprone, it will be appropriate to test these three molecules in the mouse for their ability to induce neutropenia and agranulocytosis, the most important side effect of deferiprone.

5. Experimental Section

5.1 Syntheses.

All starting materials were obtained from commercial sources and used without further purification. 5-Hydroxy-2-(hydroxymethyl)-4H-pyran-4-one (kojic acid, **11**) was purchased from Fluka. The synthesis of four of the hydroxypyridin-4-ones was achieved using previously published methods, namely **7**,[13] **9a**[7] and **10a**[14] and

10b.[15] The purity of the eight hydroxypyridinones **7**, **8a**, **8b**, **9a**, **9b**, **10a** and **10b** were all assessed by reversed phase HPLC and all were found to possess a purity of greater than 98%.

5.1.1 2-Hydroxymethyl-5-methoxy-4H-pyran-4-one (**12a**)

Kojic acid （**11**） (126.00 g, 887 mmol) was dissolved in 10% potassium hydroxide solution (620 mL) and cooled to 10^{o}C. Then dimethyl sulfate was added dropwise over 30min. The reaction mixture was stirred at 10 ^{o}C for 1h. The precipitate was collected by filtration and washed with acetone to give a white solid (**12a**) (104.3 g, 75%). ^{1}H NMR (400 MHz, DMSO-d_6) δ: 8.08 (s, 1H), 6.29 (s, 1H), 5.70 (t, *J*=6.0Hz, 1H), 4.29 (d, *J*=6.0Hz, 2H), 3.64 (s, 3H); ^{13}C NMR (100 MHz, DMSO-d_6) δ: 172.9, 168.1, 148.0, 139.0, 110.8, 59.4, 56.2.

5.1.2 5-Methoxy-4-oxo-4H-pyran-2-carboxylic acid (**13a**)

2-Hydroxymethyl-5-methoxy-4*H*-pyran-4-one (**12a**) (6.24 g, 40 mmol) was refluxed in acetone (600 mL). Jones-reagent (33 mL) was added to the solution and the reaction mixture was refluxed for 40min. The reaction mixture was cooled to room temperature. The precipitate was collected by filtration and washed with water to give a white solid (**13a**) (4.95 g, 73%). ^{1}H NMR (400 MHz, DMSO-d_6) δ: 8.27 (s, 1H), 6.90 (s, 1H), 3.69 (s, 3H), 3.37 (br, 1H); ^{13}C NMR (100 MHz, DMSO-d_6) δ: 172.7, 160.9, 152.5, 149.4, 139.6, 116.7, 56.3.

5.1.3 3-Methoxy-4H-pyran-4-one (**14a**)

5-Methoxy-4-oxo-4*H*-pyran-2-carboxylic acid (**13a**) (34.00 g, 200 mmol) and 1-methyl-2- pyrrolidinone (500 mL) were refluxed for 4h. The solvent was removed azeotropically with *N*,*N*-dimethylformamide (500 mL) in high vacuum. The residue was extracted into dichloromethane and washed with 5% aqueous sodium hydroxide (3×270 mL). The organic layer was dried over Na_2SO_4, concentrated and recrystallized from toluene to give the yellow solid (**14a**) (11.32 g, 45%). ^{1}H NMR (400 MHz, DMSO-d_6) δ: 8.12 (s, 1H), 8.10 (d, *J*=5.2Hz, 1H), 6.35 (d, *J*=5.2Hz, 1H), 3.65 (s, 3H); ^{13}C NMR (100 MHz, DMSO-d_6) δ: 172.3, 155.7, 148.8, 139.8, 115.4, 56.1.

5.1.4 3-Methoxy-4(1H)-pyridone (**15a**)

3-Methoxy-4*H*-pyran-4-one (**14a**) (3.78 g, 30 mmol) and 30% ammonia solution (40 mL, 300 mmol) were heated at 70^{o}C in 50% ethanol-water solution (50 mL) for 8h. The reaction mixture was concentrated to give product (**15a**) (3.48 g, 94%). ^{1}H NMR (400 MHz, DMSO-d_6) δ: 7.57 (d, *J*=6.4Hz, 1H), 7.47 (s, 1H), 6.17 (d, *J*=6.4Hz, 1H), 3.66 (s, 3H).

5.1.5 3-((Dimethylamino)methyl)-5-methoxy-4(1H)-pyridone (**16a**)

3-Methoxy-4(1*H*)-pyridone (**15a**) (3.13 g, 25 mmol), 40% formaldehyde (3.75 g, 50 mmol) and 40% dimethylamine (11.25 g, 100 mmol) were refluxed in ethanol (120 mL) for 72h. Then the reaction mixture was concentrated and the crude product was recrystallized from acetone/ethanol to give a white solid (**16a**) (3.52 g, 77%). ^{1}H NMR (400 MHz, DMSO-d_6) δ: 7.53 (s, 1H), 7.45 (s, 1H), 3.66 (s, 3H), 3.25 (s, 2H), 2.14 (s, 6H) ; ^{13}C NMR (100 MHz, DMSO-d_6) δ: 164.5, 148.1, 134.7, 122.6, 120.7, 56.0, 55.0, 44.9.

5.1.6 3-Methoxy-5-methyl-4(1H)-pyridone (**17**)

To 3-((dimethylamino)methyl)-5-methoxy-4(1*H*)-pyridone (**16a**) (1.46 g, 8 mmol), dissolved in absolute ethanol (60 mL) and cyclohexene (80 mL), palladium hydroxide on carbon (2 g) was added. The reaction mixture was refluxed for 5 days with further additions of cyclohexene (80 mL) and palladium hydroxide on carbon (4 g) at intervals. On cooling, the precipitate was filtered off and the filtrate was concentrated and purified by column chromatography on silica gel (eluent: CH_3OH/CH_2Cl_2 1:8) to give a white solid (**17**) (0.91 g, 81%).^{1}H NMR (400 MHz, $CDCl_3$) δ: 7.60 (s, 1H), 7.45 (s, 1H), 3.78 (s, 3H), 2.14 (s, 3H) ; ^{13}C NMR (100 MHz, $CDCl_3$) δ: 171.3, 148.4, 134.0, 123.7, 119.1, 56.2, 13.9.

5.1.7 3-Methoxy-1,5-dimethyl-4(1H)-pyridone (**18**)

To 3-methoxy-5-methyl-4(1*H*)-pyridone (**17**) (0.70 g, 5 mmol), dissolved in MeOH (20 mL), K_2CO_3 (0.76 g, 5.5 mmol) was added at room temperature and, 15min later, iodomethane (0.85 g, 6 mmol) was added. Then the reaction mixture was stirred at room temperature overnight. After completion, the reaction mixture was concentrated and the residue was purified by column chromatography on silica gel (eluent: CH_3OH/CH_2Cl_2 1:6) to give a white solid (**18**) (0.68 g, 88%). ^{1}H NMR (400

MHz, $CDCl_3$) δ: 7.13 (d, *J*=1.2Hz, 1H), 6.92 (d, *J*=2.0Hz, 1H), 3.76 (d, *J*=1.2Hz, 3H), 3.66 (s, 3H), 2.05 (s, 3H); ^{13}C NMR (100 MHz, $CDCl_3$) δ: 171.4, 148.6, 135.8, 124.7, 121.8, 56.3, 44.0, 13.8; ESI-MS m/z 154 $(M+H)^+$.

5.1.8 3-Hydroxy-1,5-dimethyl-4(1H)-pyridone hydrobromide (**8a**)

3-Methoxy-1,5-dimethyl-4(1*H*)-pyridone (**18**) (0.38 g, 2.5 mmol) was dissolved in CH_2Cl_2 (15 mL) and flushed with nitrogen. After the flask was cooled to 0 °C, tribromoborane (1M in CH_2Cl_2, 10 mL) was slowly added, and the reaction mixture was allowed to stir at room temperature for 12 h. The excess BBr_3 was eliminated at the end of the reaction by the addition of methanol (15 mL) and left to stir for another 0.5 h. After removel of the solvents under reduced pressure, the residues were purified by recrystallization from methanol/ether to afford a white solid, mp = 228^{o}C with decomposition, (0.34 g, 62%). ^{1}H NMR (400 MHz, DMSO-d_6) δ: 8.26 (s, 1H), 8.06 (d, *J*=2.0Hz, 1H), 4.04 (s, 3H), 3.57 (br, 2H), 2.17 (s, 3H) ; ^{13}C NMR (100 MHz, DMSO-d_6) δ: 158.0, 143.8, 138.7, 129.3, 123.2, 45.9, 12.8; ESI-MS m/z calc. for $C_7H_{10}NO_2$ $(M+H)^+$ 140.0706, found 140.0702.

5.1.9 5-Benzyloxy-2-hydroxymethyl-4H-pyran-4-one (**12b**)

Kojic acid (**11**) (14.20 g, 100 mmol) was dissolved in methanol (100 mL), and sodium hydroxide (4.40 g, 110 mmol) in water (10 mL) was added. The reaction mixture was heated to reflux. Then benzyl chloride (13.92 g, 110 mmol) was added dropwise over 30min and refluxed for 18h. The reaction mixture was concentrated, and dichloromethane (400 mL) was added to the residue. The inorganic salt was filtered off. The dichloromethane was washed with 5% sodium hydroxide solution (100 mL), water (100 mL), dried over Na_2SO_4, filtered, concentrated and recrystallized from ethanol to give a pale yellow solid (**12b**) (19.26 g, 83%).

5.1.10 5-Benzyloxy-4-oxo-4H-pyran-2-carboxylic acid (**13b**)

5-Benzyloxy-2-hydroxymethyl-4*H*-pyran-4-one (**12b**) (10.00 g, 43 mmol) was dissolved in acetone (1000 mL). Jones-reagent (25 mL) was added to the solution and the reaction mixture was stirred below 20^{o}C for 3h. The precipitate was filtered off. The filtrate was concentrated to dryness and the crude product was recrystallized from methanol to give white crystals (**13b**) (8.51 g, 80%).

5.1.11 3-Benzyloxy-4H-pyran-4-one (**14b**)

5-Benzyloxy-4-oxo-4*H*-pyran-2-carboxylic acid (**13b**) (15.87 g, 64.5 mmol) and 1-methyl-2- pyrrolidinone (160 mL) were refluxed for 4h. Then the solvent was removed azeotropically with *N*,*N*-dimethylformamide (160 mL) in high vacuum. The residue was extracted into dichloromethane and washed with 5% aqueous sodium hydroxide (3×90 mL). The organic layer was dried over Na_2SO_4, concentrated and recrystallized from toluene to give a pale yellow solid (**14b**) (9.07 g, 70%).

5.1.12 3-Benzyloxy-4(1H)-pyridone (**15b**)

3-Benzyloxy-4*H*-pyran-4-one (**14b**) (7.90 g, 39 mmol) and 30% ammonia solution (52 mL, 390 mmol) were heated at 70^{o}C in 50% ethanol-water solutuion (60 mL) for 24h. Then the reaction mixture was cooled to room temperature. The precipitate was collected by filtration to give a white solid (**15b**) (6.98 g, 89%).

5.1.13 3-Benzyloxy-5-((dimethylamino)methyl)-4(1H)-pyridone (**16b**)

3-Benzyloxy-4(1*H*)-pyridone (**15b**) (3.02 g, 15 mmol), 40% formaldehyde (2.25 g, 30 mmol) and 40% dimethylamine (6.75 g, 60 mmol) were refluxed in ethanol (100 mL) for 72h. Then the reaction mixture was concentrated and the crude product was recrystallized from acetone/ethanol to give a white solid (**16b**) (2.76 g, 71%). ^{1}H NMR (400 MHz, DMSO-d_6) δ: 7.52-7.50 (m, 2H), 7.42-7.35 (m, 5H), 5.00 (s, 2H), 3.23 (s, 2H), 2.14 (s, 6H); ^{13}C NMR (100 MHz, DMSO-d_6) δ: 169.8, 146.7, 137.3, 134.9, 128.4, 128.0, 127.9, 123.8, 123.6, 70.5, 55.1, 45.0.

5.1.14 3-Hydroxy-5-methyl-4(1H)-pyridone hydrochloride (**8b**)

To 3-benzyloxy-5-((dimethylamino)methyl)-4(1*H*)-pyridone (**16b**) (1.00 g, 3.9 mmol), dissolved in absolute ethanol (30 mL) and cyclohexene (40 mL), palladium hydroxide on carbon (1 g) was added. The reaction mixture was refluxed for 5 days with further additions of cyclohexene (40 mL) and palladium hydroxide on carbon (2 g) at intervals and then cooled. The catalysts were filtered off. The filtrate was acidified with hydrochloric acid, concentrated and purified by column chromatography on silica gel (eluent: CH_3OH/CH_2Cl_2 1:7) to give a white solid, mp = 237-238^{o}C (**8b**) (0.47 g, 75%).^{1}H NMR (400 MHz, DMSO-d_6) δ: 8.13 (s, 1H), 8.07 (s, 1H), 2.18 (s, 3H) ; ^{13}C NMR (100 MHz, DMSO-d_6) δ: 170.7, 145.8, 131.8,

120.4, 117.2, 13.2; ESI-MS m/z calc. for $C_6H_8NO_2$ $[M+H]^+$ 126.0550, found 126.0552.

5.1.15 5-Hydroxy-2-methyl-4H-pyran-4-one (**20a**) was synthesized from kojic acid in two steps using a previously published procedure.[20]

5.1.16 5-Benzyloxy-2-methyl-4H-pyran-4-one (**20b**)

5-Hydroxy-2-methyl-4*H*-pyran-4-one (**20a**) (3.78 g, 30 mmol) was dissolved in methanol (30 mL), and sodium hydroxide (1.32 g, 33 mmol) in water (3 mL) was added. The reaction mixture was heated to reflux. Then benzyl chloride (4.18 g, 33 mmol) was added dropwise and refluxed for 4h. The reaction mixture was concentrated, and dichloromethane (150 mL) was added to the residue. The inorganic salt was filtered off. The dichloromethane was washed with 5% sodium hydroxide solution (30×2 mL), water (30 mL), dried over Na_2SO_4, filtered, concentrated and recrystallized from dichloromethane/petroleum ether to give a white solid (**20b**) (5.25 g, 81%). ^{1}H NMR (400 MHz, $CDCl_3$) δ: 7.46 (s, 1H), 7.41-7.32 (m, 5H), 6.21 (s, 1H), 5.07 (s, 2H), 2.31 (s, 3H); ^{13}C NMR (100 MHz, $CDCl_3$) δ: 174.8, 165.0, 146.7, 141.6, 135.9, 128.6, 128.3, 127.8, 114.3, 71.8, 19.6.

5.1.17 5-Benzyloxy-2-methyl-4(1H)-pyridone (**21**)

5-Benzyloxy-2-methyl-4*H*-pyran-4-one (**20b**) (4.32 g, 20 mmol) and 30% ammonia solution (26 mL, 200 mmol) were heated at 70^{o}C in 50% ethanol-water solution (30 mL) for 48h. Then the reaction mixture was cooled to room temperature. The precipitate was collected by filtration to give a white solid (**21**) (4.02 g, 93%). ^{1}H NMR (400 MHz, DMSO-d_6) δ: 11.21 (br, 1H), 7.9-7.31 (m, 6H), 6.00 (s, 1H), 4.97 (s, 2H), 2.16 (s, 3H); ESI-MS m/z 216 $[M+H]^+$.

5.1.18 5-Hydroxy-2-methyl-4(1H)-pyridone hydrochloride (**9b**)

Palladium (5%) on carbon (0.12 g) was added to the solution of 5-benzyloxy-2-methylpyridin-4(1*H*)-one (**21**) (1.08 g, 5 mmol) in methanol (20 mL). The reaction mixture was subjected to hydrogenolysis for 3.5h. The catalysts were filtered off. The filtrate was acidified with concentrated hydrochloride acid, concentrated and recrystallized from methanol/diethyl ether to give a white solid, mp = 183-184^{o}C (**9b**) (0.73g, 90%). ^{1}H NMR (400 MHz, DMSO-d_6) δ: 8.00 (s, 1H),

7.12 (s, 1H), 2.48 (s, 3H); ^{13}C NMR (100 MHz, DMSO-d_6) δ: 161.0, 145.9, 143.4, 125.8, 112.4, 18.2; ESI-MS m/z calc. for $C_6H_8NO_2$ $[M+H]^+$ 126.0550, found 126.0548.

5.2 Physical Measurements

^{1}H NMR spectra were recorded using a Bruker 360 MHz NMR spectrometer. Chemical shifts are reported in ppm.

Mass spectra (ESI) analyses were carried out by the Mass Spectrometry Facility, School of Biomedical Sciences, 150 Stamford Street London, SE1 9NH, U.K.

For pK_a determinations, an automatic titration system comprising an autoburet (Metrohm Dosimat 765, 1 mL syringe) and a Mettler Toledo MP230 pH meter with a Metrohm pH electrode (6.0133.100) and a reference electrode (6.0733.100) was used. A 0.1 M KCl electrolyte solution was used to maintain the ionic strength. For the measurements the temperature of the probe solution was maintained in a thermostatic jacketed titration vessel at 2.5 ± 0.1 ^{o}C using a Teghne TE-8J temperature controller. The solution was stirred vigorously during the experiment. A Gilson Mini-plus#3 pump with speed capability (20 mL/min) was used to circulate the probe solution through a Hellem quartz flow cuvette. A cuvette path length of 10 mm was used and the flow cuvette mounted on a HP 8453 UV – visible spectrophotometer. All instruments were interfaced to a computer and controlled by a Visual Basic program. The pH of the probe solution was increased by 0.1 pH unit by the addition of KOH from the autoburet. When pH readings varied by <0.001 pH unit over a 3 s period, an incubation period of 1 min was adopted. At the end of the equilibrium period, the spectrum of the solution was recorded. The cycle was repeated automatically until the defined end point pH value was achieved. Titration data were analyzed by pHab.[21]

5.2.1 pKa Determination.

The pH electrodes were calibrated by titrating a volumetric standard strong acid HCl (0.15 mL, 0.2092 M) in KCl (15 mL, 0.1 M) with KOH (0.1 M) under an argon atmosphere at 25 ^{o}C. The E_0, slope of the electrode, and pK_w of the solution were both optimized by GLEE.[22] Following electrode calibration, a 1 mM solution of

ligand in 00.162 mL of 0.1 M KCl at an initial pH value of 1.646 were alkalimetrically titrated to pH 11.162. The spectra of the ligands and the titration experimental data at different pH values were analyzed by refining the extinction coefficients of the protonated and deprotonated species.

5.2.2 Fe^{3+} Stability Constant Determination.

For the stability constant determinations, a 50mm path length cuvette was used. Automatic titration and spectral scans adopted the following strategy: the pH of a solution was increased by 0.1 pH unit by the addition of KOH from the autoburette; when pH readings varied by <0.001 pH unit over a 3s period, an incubation period was activated. For stability constant determinations, a period of 5 min was adopted. At the end of the equilibrium period, the spectrum of the solution was recorded. The cycle was repeated automatically until the defined end point pH value was achieved. All the titration data were analyzed with the pHab program.[21] The species plot was calculated with the HYSS program.[22] Analytical grade reagent materials were used in the preparation of al solutions. pFe^{3+} conditions were $[Fe^{3+}]_{Total}$ = 1 µM; $[Ligand]_{Total}$ = 10 µM, pH = 7.4.

5.2.3 LogP Determination.

The logP values of both the ligands and the corresponding 1:3 complexes were determined by the shake-flask method using a *n*-octanol-aqueous system at 25°C. Because the logP is strictly defined for neutral molecules, the partition studies were undertaken in MOPS (25 mM, pH 7.4). The absorbance of a buffered probe solution of known concentration was recorded spectrophotometrically, and different ratios of buffered probe solution and *n*-octanol were then shaken by vigorous stirring for 15 sec. The layers were subsequently separated by centrifugation at 25°C. The aqueous phases were again measured spectrophotometrically showing a decrease of probe absorbance due to partition into the organic phase. Lipophilicity, directly correlating with the detected decrease in probe absorbance, was derived from the recorded UV spectra according to the following equation:

$$P = \frac{(A_0-A_1)V_{aq}}{A_1V_o}$$

Where A_0 is the initial absorbance of the aqueous phase, A_1 is the absorbance of the aqueous phase after partition.

5.3 Metabolism of 3-hydroxypyridin-4-ones

Individual hydroxypyridinones (10 μM) were incubated with 1mg/mL UltraPool™ Human Liver Microsome (HLM) 150 Mixed Gender Pooled, Cat No. 452117 (Corning Ltd-Life Sciences, Ewole, UK) with the add-in of Phase I or Phase I&II Corning NADPH and UDPGA system solutions (Corning Ltd-Life Sciences, Ewloe, UK)) in 100mM PBS buffer. NADPH regenerating system solution A (Cat No. 451220, Lot No. 3189637), NADPH regenerating system solution B (Cat No. 451200, Lot No. 3246566), UGT reaction mix solution A (UDPGA Cofactor) (Cat No. 451300, Lot No. 3211810), UGT reaction mix solution B (5X-UGT Buffer Mix with Alamethicin) (Cat No. 451320, Lot No. 3211815). Blanks were prepared the same way except that HLM was excluded in incubates. 500μL incubation solutions were prepared with one single blank and triplicate sample solutions for each HPO compound. Solutions were incubated at 37°C in for 24hrs with gentle shaking to prevent protein sedimentation. The reactions were terminated by spiking in 400μL 4% phosphoric acid, followed by spiking in 100μL of 100μM CP21 as the internal standard. Samples were mixed evenly by the vortex mixer and followed by centrifuge at 14,000 rpm in a Spectrafuge™ 16M microcentrifuge (Labnet International Inc., NJ, USA) for 10min. The supernatants were collected for the further solid phase extraction. OASIS MCX (Mixed-Mode Cation-exchange) 96-well μElution Plate, 2 mg sorbent per well, 30 μm Particle Size (Oasis®, Waters, UK) was applied to extract the parent HPO compounds and their metabolites with a high throughput Supelco® SPE PlatePrep vacuum manifold (Sigma-Aldrich, UK).

Sample plates after SPE were subjected to a Waters Acquaity UPLC- Xevo™ TQ MS system (Waters Limited, Elstree, UK) to further identify the major metabolites and quantify the percentage of drug metabolized after 24hrs incubation. The Agilent Poroshell 120 EC-C18 column, 2.1 x 50mm 2.7μm (Agilent Technologies LDA UK Limited, Lakeside, UK) was applied for separation. A 9 min gradient UPLC

condition was used from 10% to 90% mobile phase B for 4 min, equilibrated at 90% B for 1.5min, followed by 0.1 min gradient from 90% to 10% B and held at 10% B for another 3.4min with the mobile phases consisted of A: PFOA (1g) in 0.1% formic acid, 95% ACN, 5% H_2O and B: PFOA (1g) in 0.1% formic acid, 95% H_2O, 5% ACN. The coupled MS was operated at positive ion electrospray mode.

The percentages of drug metabolized were calculated using the Microsoft Excel software and the data were plotted into a bar chart using GraphPad Prism 6.

Acknowledgements

YYX wishes to acknowledge the National Natural Science Foundation of China (#21576239) for financial support to visit King's College London for a 12 month period. We also wish to thank Mr Effychios Manoli for his assistance with the running and interpretation of the mass spectral data.

Abbreviations:

density functional theory, DFT; mass spectroscopy, MS; dimethyl sulfoxide, DMSO; electrospray ionization, ESI; 3-morpholinopropanesulfonic acid, MOPS; human liver microsome, HLM; solid phase extraction, SPE; acetonitrile, ACN; pentadecafluorooctanoic acid, PFOA

References:

1. A. Maggio, G.D'Amico, A. Morabito, M. Capra, C. Ciaccio, P. Cianciulli, Deferiprone versus desferrioxamine in patients with thalassemia major: a randomized clinical trial. Blood Cells, Molecules, and Disease. **28** (2002): 196-208.
2. A.Taher， E.Aoun, A.I. Sharara, F. Mourad, W. Gharzuddine, S. Koussa, A. Inati, A. P. Dhillon, A.V.Hoffbrand, Five-Year Trial of Deferiprone Chelation Therapy in Thalassaemia major Patients, Acta Haematologia **112** (2004) 179-183.
3. D.J. Pennell, J. B. Porter, M. D.Cappellini, *et al*, Tailoring Iron Chelation By Iron Intake And Serum Ferritin: The Prospective EPIC Study Of Deferasirox In 1744 Patients With Transfusion-Dependent Anemias, *Haematologica* **95** (2010) 557-566.
4. A. J. Baksi, and D. J. Pennell, Randomized controlled trials of iron chelators for the treatment of cardiac siderosis in thalassaemia major. *Frontiers in Pharmacology* **5** (2014) 217-220.
5. Y. Ma, T. Zhou, X. Kong, R. C. Hider, Chelating Agents for the Treatment of Systemic Iron Overload. *Curr. Med. Chem.* **19** (2012) 2816-2827.
6. R. C. Hider, X. Kong, Iron speciation in the cytosol: an overview. *Dalton Trans* **42** (2013) 3220-3229.
7. S. Singh, R. O. Epemolu, P. S. Dobbin, G. S. Tilbrook, B. L. Ellis, L. A. Damani, R. C. Hider, Urinary metabolic profiles in human and rat of 1,2-dimethyl- and 1,2-diethyl-substituted 3-hydroxypyridin-4-ones. *Drug Metabol and Disposition* **20** (2002) 256-261.
8. A. Ceci, P. Baiardi, *et al*, The safety and effectiveness of deferiprone in a large-scale, 3-year study in Italian patients. *Brit. J.Haematology* **118** (2002) 330-336.
9. Neufeld E. J., Oral chelators deferasirox and deferiprone for transfusional iron overload in thalassemia major: new data, new questions, *Blood* **107** (2006) 3436-3441.

10. Y. Ma, X. Kong, Y. Chen, R. C. Hider, Synthesis and characterization of pyridazine-based iron chelators. *Dalton Trans.* **43** (2014) 17120-17128.
11. Y. Ma, R. C. Hider, Design and synthesis of fluorine-substituted 3-hydroxypyridin-4-ones, *Tet. Letts.* **51** (2010) 5230-5233.
12. Y. Ma, Y. Xie; R. C. Hider, A novel fluorescence method for determination of $pFe^{(3+)}$., *Analyst* **138** (2013) 96-99.
13. P. S. Dobbin, R. C. Hider, A. D. Hall, P. D. Taylor, P. Sarpong, J. B. Porter, G. Xiao, D. van der Helm, Synthesis, physicochemical properties, and biological evaluation of N-substituted 2-alkyl-3-hydroxy-4(1H)-pyridinones: orally active iron chelators with clinical potential, *J. Med. Chem.* **36** (1993) 2448-2458.
14. Y. L. Chen, D. J. Barlow, X. Kong, Y. Ma, R. C.Hider, Prediction of 3-hydroxypyridin-4-one (HPO) hydroxyl pK(a) values. *Dalton Trans* **41** (2012) 6549-6557.
15. Y. L. Chen, D. J. Barlow, X. Kong, Y. Ma, R. C.Hider, Prediction of 3-hydroxypyridin-4-one (HPO) log K-1 values for Fe(III). *Dalton Trans* **41** (2012), 10784-10791.
16. B. L. Rai, L. S. Dekhordi, H. Khodr, Y. Jin, Z. Liu, R. C. Hider, Synthesis, physicochemical properties and evaluation of N-substituted-2-alkyl-3-hydroxy-4(1H)-pyridinones. , *J. Med. Chem.* **41** (1998) 3347-3359.
17. Gaussian 09, Revision **D.01**, M. J. Frisch, G. W. Trucks, H. B. Schlegel, G. E. Scuseria, M. A. Robb, J. R. Cheeseman, G. Scalmani, V. Barone, B. Mennucci, G. A. Petersson, H. Nakatsuji, M. Caricato, X. Li, H. P. Hratchian, A. F. Izmaylov, J. Bloino, G. Zheng, J. L. Sonnenberg, M. Hada, M. Ehara, K. Toyota, R. Fukuda, J. Hasegawa, M. Ishida, T. Nakajima, Y. Honda, O. Kitao, H. Nakai, T. Vreven, J. A. Montgomery, Jr., J. E. Peralta, F. Ogliaro, M. Bearpark, J. J. Heyd, E. Brothers, K. N. Kudin, V. N. Staroverov, R. Kobayashi, J. Normand, K. Raghavachari, A. Rendell, J. C. Burant, S. S. Iyengar, J. Tomasi, M. Cossi, N. Rega, J. M. Millam, M. Klene, J. E. Knox, J. B. Cross, V. Bakken, C. Adamo, J. Jaramillo, R. Gomperts, R. E. Stratmann, O. Yazyev, A. J. Austin, R. Cammi, C. Pomelli, J. W.

Ochterski, R. L. Martin, K. Morokuma, V. G. Zakrzewski, G. A. Voth, P. Salvador, J. J. Dannenberg, S. Dapprich, A. D. Daniels, Ö. Farkas, J. B. Foresman, J. V. Ortiz, J. Cioslowski, and D. J. Fox, Gaussian, Inc., Wallingford CT, 2009.

18. E. G. Hohenstein, C. D. Sherrill, Effects of Heteroatoms on Aromatic π−π Interactions: Benzene−Pyridine and Pyridine Dimers, *J. Phys. Chem. A.* **113** (2009) 878-886.
19. J. B. Porter, R. D. Abeysinghe, K. P. Hoyes, C. Barra, E. R. Huehns, P. N. Brooks, M. P. Blackwell, M. Araneta, G. Brittenham, S. Singh, P. Dobbin，R. C. Hider，Contrasting interspecies efficacy and toxicology of 1, 2-diethyl-3 -hydroxypyridin-4-one, CP94, relates to differing metabolism of the iron chelating site. *Brit. J. Haematotl.* **85** (1993) 159-168.
20. B. L. Ellis, A. K. Duhme, R. C. Hider, M. B.Hossain, S.Rizvi, D. van der Helm, Synthesis, Physicochemical Properties, and Biological Evaluation of Hydroxypyranones and Hydroxypyridinones: Novel Bidentate Ligands for Cell-Labeling, *J. Med. Chem.* **39** (1996) 3659-3670.
21. P. Gans, A. Sabatini, Determination of equilibrium constants from spectrophometric data obtained from solutions of known pH: The program pHab. *Ann. Chim.* **89** (1999) 45–49.
22. L. Alderighi, P. Gans, A. Ienco, D. Peters, A. Sabatini, A. Vacca; Hyperquad simulation and speciation (HySS): a utility program for the investigation of equilibria involving soluble and partially soluble species; *Coord. Chem. Rev.* **184** (1999) 311–318.

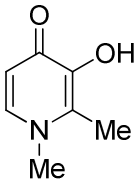

1

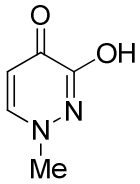

2

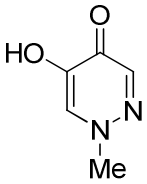

3

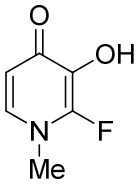

4

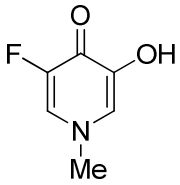

5

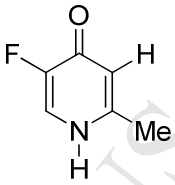

6

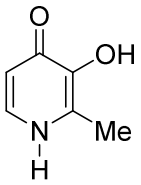

7

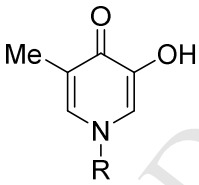

8a, R = Me
8b, R = H

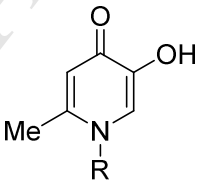

9a, R = Me
9b, R = H

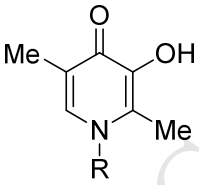

10a, R = Me
10b, R = H

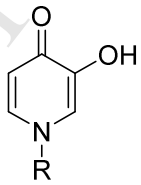

22

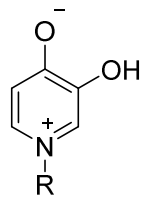

23

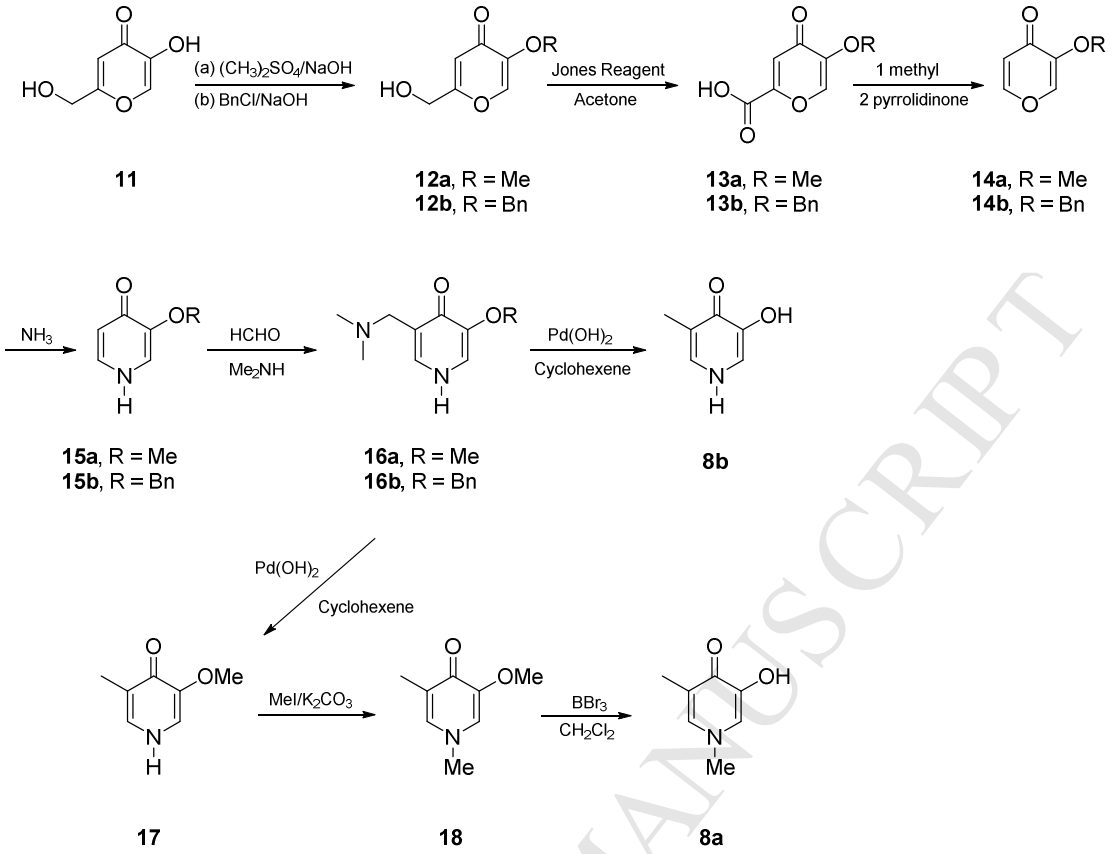

Scheme 1 Synthetic routes for **8a** and **8b**

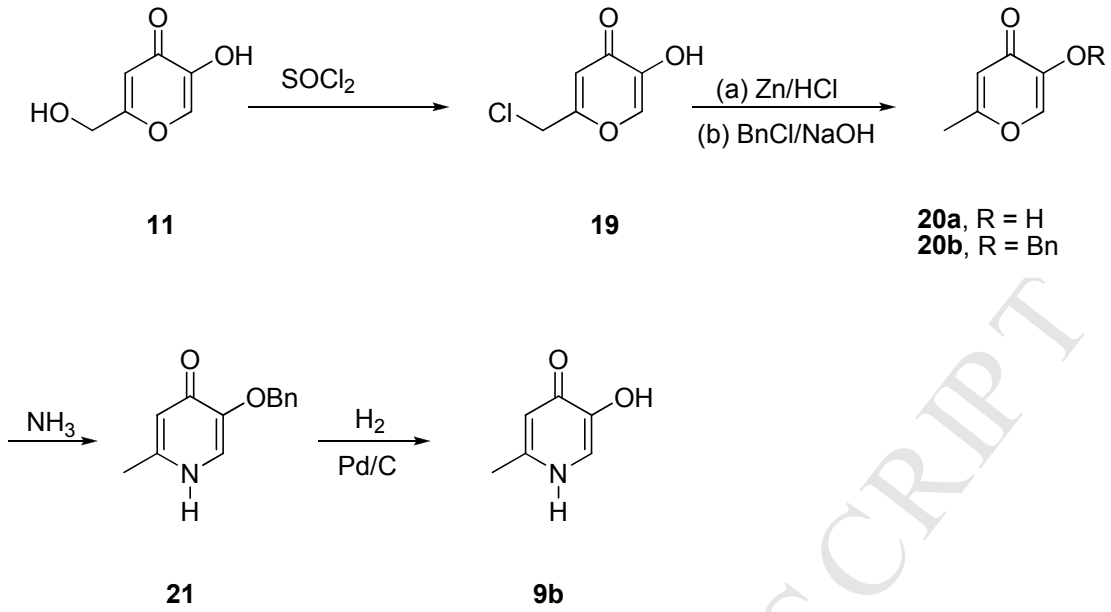

Scheme 2 Synthetic route for **9b**

Table 1 Physicochemical parameters for 3-hydroxypyridin-4-ones.

Compound	pKa_1	pKa_2	$logK_1$	$log\beta_2$	$log\beta_3$	pFe^{3+}	$logP_{(ligand)}$	$logP_{(iron\ complex)}$
Deferiprone (**1**)	3.61	9.78	15.03	27.42	37.35	20.74	-0.77	-2.60
(**8a)**	3.31	9.34	14.34	26.22	35.76	20.46	-0.93	-2.69
(**9a**)	3.64	9.13	13.96	25.62	35.07	20.39	-1.19	-3.63
(**10a**)	3.37	10.32	15.51	28.12	37.93	19.71	-0.51	-1.86
(**7**)	3.64	9.73	14.79	26.96	36.63	20.17	-0.58	-2.46
(**8b**)	3.31	9.49	14.41	26.31	35.80	20.06	-0.59	-2.03
(**9b**)	3.60	9.32	14.18	25.92	35.37	20.13	-0.73	-2.00
(**10b**)	3.43	10.27	15.35	27.75	37.28	19.22	-0.13	-1.08

Figure Legends

Figure 1. Spectrophotometric titration of 3-hydroxy-5-methyl-4(1*H*)-pyridone (**8b**). A, titration of free ligand (**8b**) over the range pH 1.6-11.0; B, titration of (**8b**) in the presence of iron(III) (5:1, molar ratio) over the range pH 1.2-8.0; C, speciation plot of iron(III)·**8b** complexes; [Fe^{III}] = 1µM; [**8b**] = 10µM.

Figure 2. Relationship between logD values (pH 7.4) of free ligands and their corresponding (3:1) iron(III) complexes.

Figure 3. Percentage contribution of zwitterionic mesomers (**23**) for 3-hydroxypyridin-4-ones; □,*in vacuo*; ■, in water.

Figure 4. ESI mass spectrum of deferiprone (**1**) presented as aqueous solution (pH 7.4, 140µM); dimer, 279.0; monomer, 140.17.

Figure 5. Influence of hydroxypyridin-4-one concentration on dimerisation.
Dimerisation recorded by peak height ratio of species in mass spectra.

Figure 6. Metabolic conversion of 3-hydroxypyridin-4-ones by human liver microsomes; black bar: phase 1 metabolism; grey bar: phase 1 and phase 2 metabolism

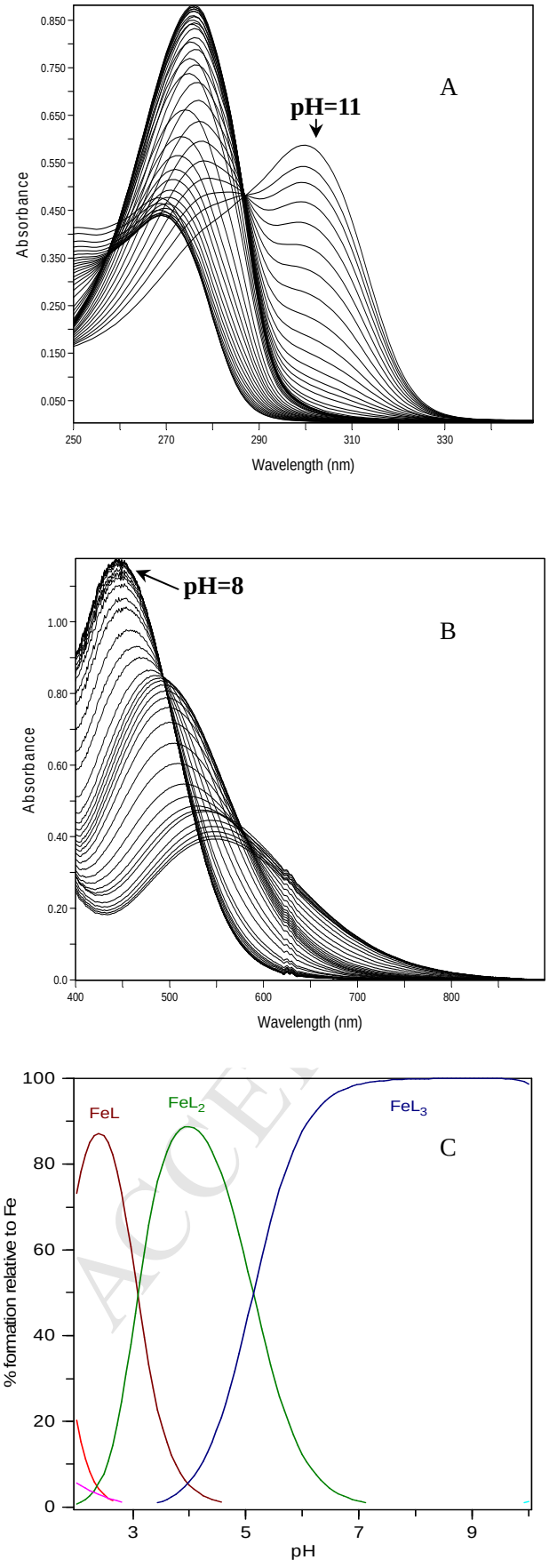
A
pH=11
Absorbance
Wavelength (nm)
B
pH=8
Absorbance
Wavelength (nm)
C
FeL
FeL2
FeL3
% formation relative to Fe
pH

Figure 1.

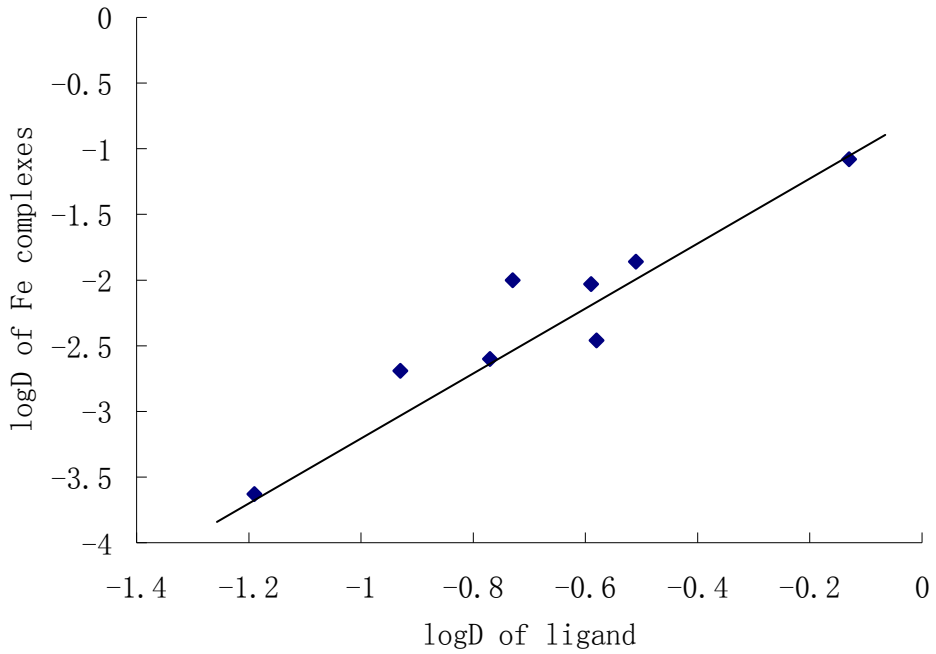

Figure 2

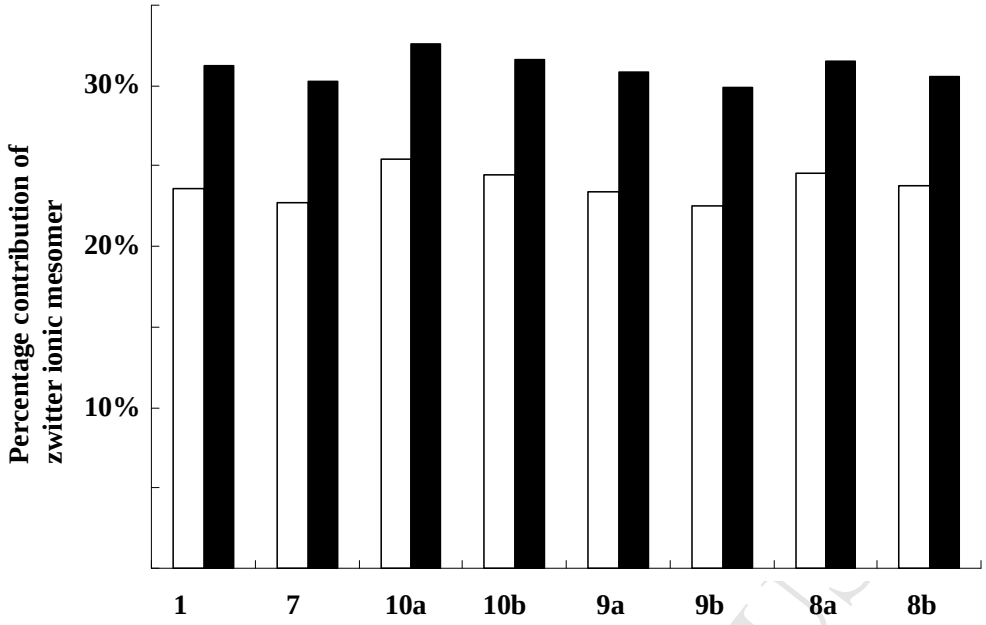

Figure 3.

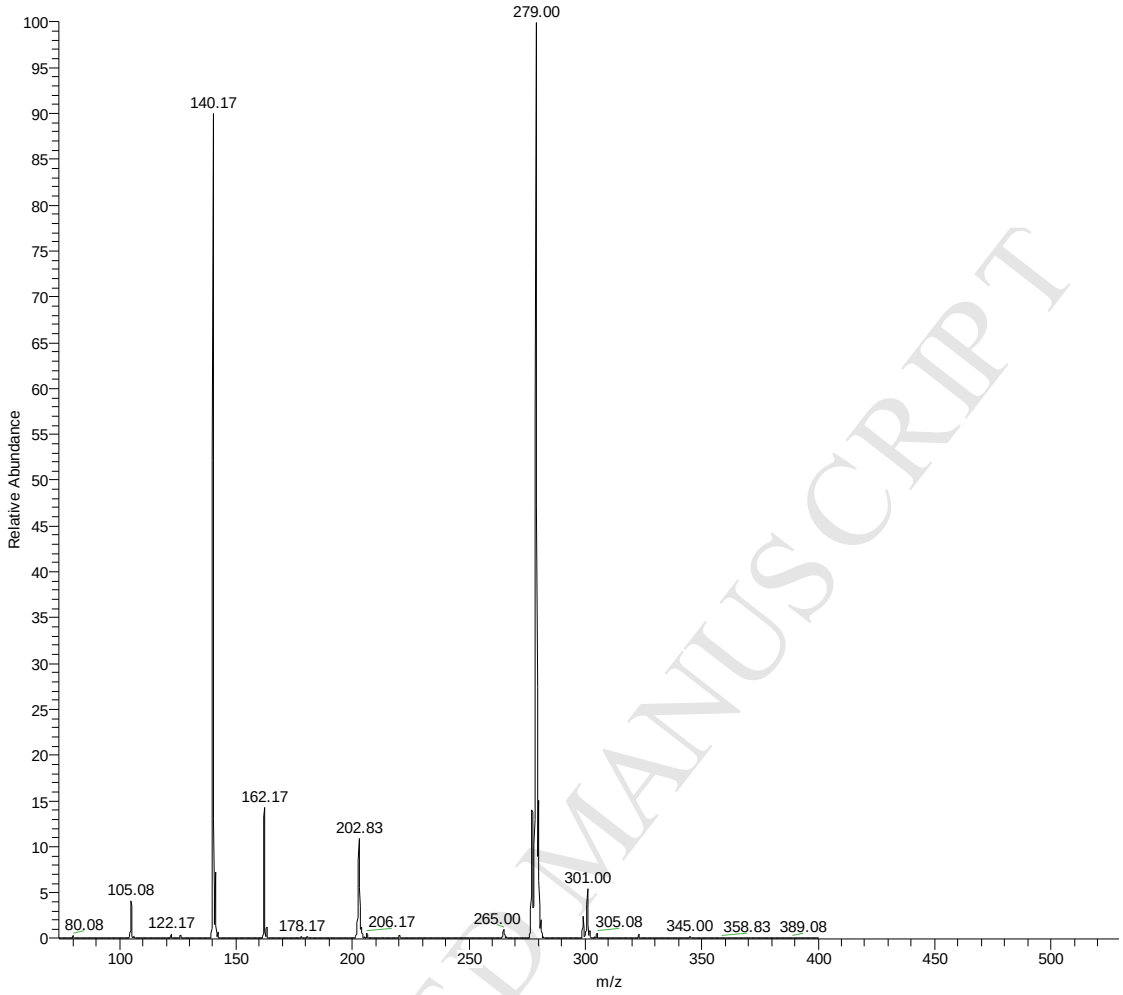

Figure 4

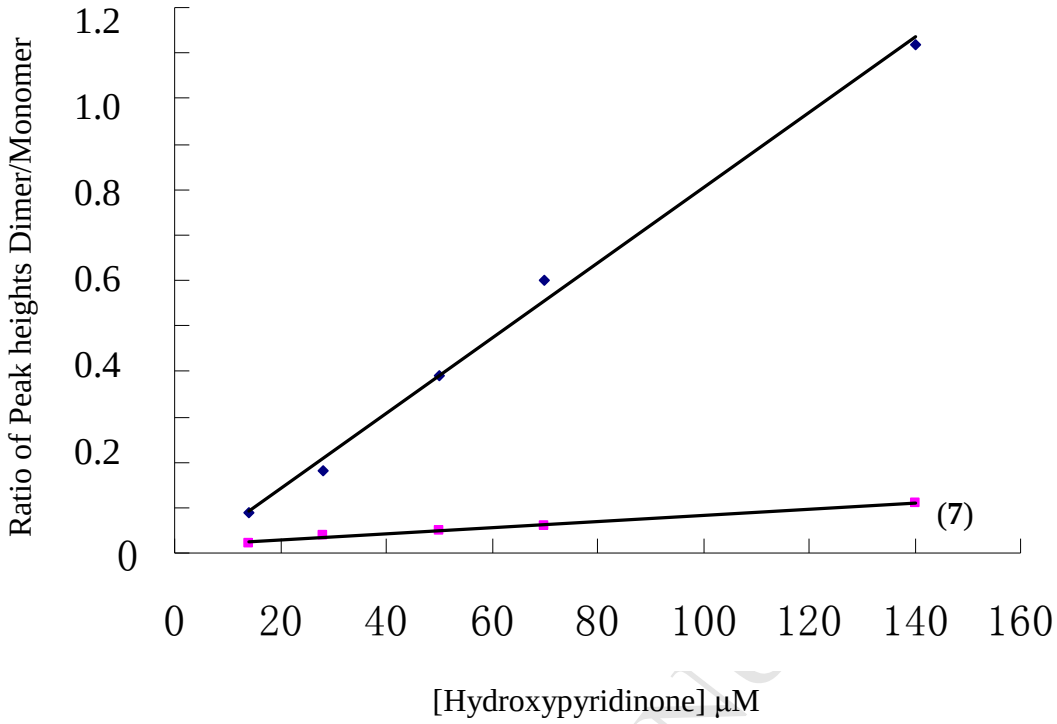

Figure 5

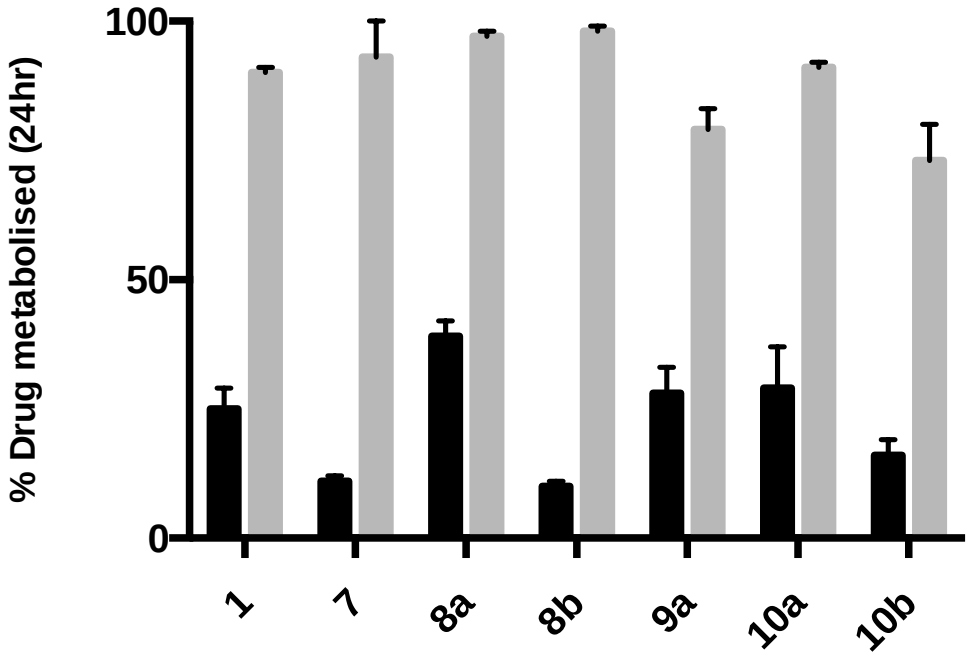

Figure 6